LABORATORY INVESTIGATION

EGCG inhibits properties of glioma stem-like cells and synergizes with temozolomide through downregulation of P-glycoprotein inhibition

**Yong Zhang · Shao-Xiang Wang · Ji-Wei Ma ·
Hai-Ying Li · Jie-Cheng Ye · Si-Ming Xie ·
Bin Du · Xue-Yun Zhong**

Abstract Rational: Combination therapy to inhibit cancer stem cells may have important clinical implications. Here, we examine the molecular mechanisms by which epigallocatechin gallate (EGCG), a bioactive polyphenol in green tea, inhibits the stem cell characteristics of glioma stem-like cells (GSLCs) and synergizes with temozolomide (TMZ), a DNA-methylating agent commonly used as first-line chemotherapy in gliomas. GSLCs were enriched from the human glioblastoma cell line U87 using neurosphere culture. Cells were analyzed using flow cytometry, quantitative PCR, and western blotting. Compared to U87 cells, a higher percentage of U87 GSLCs remained in the G0/G1 phase, with downregulation of the cell-cycle protein CylinD1 and overexpression of stem cell markers CD133 and ALDH1. The drug-resistance gene ABCB1 (but not ABCG2 or MGMT) also showed high mRNA and protein expression. The resistance index of U87 GSLCs against TMZ and carmustine (BCNU) was 3.0 and 16.8, respectively. These results indicate that U87 GSLCs possess neural stem cell and drug-resistance properties. Interestingly, EGCG treatment inhibited cell viability, neurosphere formation, and migration in this cell model. EGCG also induced apoptosis, downregulation of p-Akt and Bcl-2, and cleaving PARP in a dose-dependent manner. Importantly, EGCG treatment significantly downregulated P-glycoprotein expression but not that of ABCG2 or MGMT and simultaneously enhanced sensitivity to TMZ. Our study demonstrates that the use of EGCG alone or in combination with TMZ may be an effective therapeutic strategy for glioma.

Keywords EGCG · Neurosphere culture · Temozolomide · Glioma · P-gp · Stem cell

Yong Zhang and Shao-Xiang Wang contributed equally to this study.

Y. Zhang · S.-X. Wang · J.-W. Ma · H.-Y. Li · J.-C. Ye ·
S.-M. Xie · B. Du (✉) · X.-Y. Zhong
Department of Pathology, Medical School of Jinan University,
Guangzhou 510632, People's Republic of China
e-mail: tdubin@jnu.edu.cn

Y. Zhang · S.-X. Wang · J.-W. Ma · H.-Y. Li · J.-C. Ye ·
S.-M. Xie · B. Du · X.-Y. Zhong (✉)
Guangdong Province Key Laboratory of Molecule Immunology
and Antibody Engineering, Jinan University,
Guangzhou 510632, China
e-mail: tzxy@jnu.edu.cn

S.-X. Wang
School of Medicine, Shenzhen University, Shenzhen 518060,
China

Introduction

Gliomas are the most common tumors of the central nervous system (CNS), accounting for more than 30 % of all malignant CNS tumors. Conventional therapies, including chemotherapy, play an important role in glioma management. Carmustine (BCNU) has been a commonly used chemotherapeutic agent to treat gliomas for many years [1]. Recently, temozolomide (TMZ) has been utilized as an alternative therapy to treat malignant gliomas [2]. However, the 5-year survival rate of glioma patients is still fairly low, primarily because these chemotherapy drugs display little efficacy toward glioma stem-like cells (GSLCs). Cancer stem-like cells have been reported to be the only tumorigenic population in GBM, as the unlimited proliferation potential of these cells supports tumor

development and maintenance [3]. Thus, appropriate strategies to eliminate GSLCs may facilitate the identification of novel therapeutic approaches for glioma treatment.

Previous studies have shown that GSLCs overexpress many drug-resistance proteins, which underlie glioma's resistance to conventional chemotherapy agents. These drug-resistance proteins include ATP-binding cassette (ABC) and O^6-methylguanine–DNA methyltransferase DNA repair protein (MGMT) [4–6]. ABC transporters, such as P-glycoprotein (P-gp) and breast cancer resistance protein (BCRP, also known as ABCG2), stimulate efflux of cytotoxic drugs, leading to multidrug resistance. The MGMT enzyme repairs DNA breakage caused by alkylating agents, such as TMZ. Downregulating these resistance-associated proteins reverses drug resistance in multiple cancer cells [7–9]. Thus, the inhibition of drug-resistance proteins in GSLCs may be a promising strategy for glioma therapy.

Epigallocatechin gallate (EGCG), a major catechin in green tea, has chemo-sensitizing effects on a wide range of malignancies, including inhibition of cancer cell growth, invasion, angiogenesis, and metastasis [10, 11]. EGCG can be used to reverse drug resistance; treatment can induce apoptosis and inhibit expression of P-gp and ABCG2 in drug-resistant cancer cells of the ovaries, breast, and lung [12–14]. However, neither the effects of EGCG in GSLCs, nor its potential mechanisms of action have been evaluated. In this study, we enriched for GSLCs from the U87 cell line and characterized their stem-like behavior. Furthermore, we found that EGCG inhibited the growth of U87 GSLCs and decreased expression of P-gp, thereby reversing resistance to TMZ. Thus, this study indicates that EGCG could potentially be used as a novel drug for the treatment of GSLCs.

Materials and methods

Cell culture

Human glioblastoma cell lines U87, U251, and SHG-44 and the rat glioma cell line C6 were obtained from the Shanghai Institute of Cell Biology, Chinese Academy of Sciences (Shanghai, China). All cells were cultured in Dulbecco's modified Eagle medium (DMEM; Gibco Life Technologies, Paisley, Scotland, UK) supplemented with 10 % fetal bovine serum, 100 IU/ml penicillin, and 100 mg/ml streptomycin. Cells were maintained in an atmosphere of 5 % CO_2 at 37 °C.

Neurosphere culture

Glioblastoma cells were plated in a 60-mm dish (Costar Corning, NY, US) at a density of 5,000 cells/ml in serum-free DMEM/F12 supplemented with B27 (Invitrogen, San Diego, CA), 20 ng/ml human basic fibroblast growth factor (Sigma-Aldrich, Taufkirchen, Germany), and 20 ng/ml epidermal growth factor (Invitrogen, Carlsbad, CA, USA). Cells were maintained at 37 °C in a humidified atmosphere of 95 % air and 5 % CO_2. Spheroids were collected after 7 days and dissociated with Accutase (a mixture of enzymes with proteolytic, collagenolytic, and DNase activity; Invitrogen, Carlsbad, CA). The cells obtained from dissociation were filtered through a 40-μm cell strainer and cell number was quantified with a Coulter counter using trypan blue dye.

Cytotoxicity assays with Cell Counting Kit-8 (CCK-8)

The effects of BCNU (Tianjin Drug Factory, Tianjin, China), TMZ (Sigma-Aldrich, St. Louis, MO, USA), Verapamil (Sigma-Aldrich, USA), and EGCG (Sigma-Aldrich, St. Louis, MO, USA) were measured using the CCK-8 assay (Dojindo Laboratories, Kumamoto, Japan). Cells were seeded into 96-well plates at a density of 5×10^3 cells per well. Various doses of BCNU, TMZ, or EGCG were added to each well 24 h after seeding. Optical density at 450-nm was measured using a microplate reader (Winooski, VT, USA). The IC_{50} value, determined by the relative absorbance of CCK-8, was assessed using probit regression analysis in SPSS 13.0 statistical software. The resistance index (RI) was calculated by normalizing the IC_{50} of the resistant cell line to that of the parental cell line [15].

Cell cycle assay

The cells were treated with DMEM without fetal bovine serum for 24 h, then washed with phosphate buffered saline (PBS), trypsinized, and resuspended in ice-cold PBS. The cells were then gently pelleted by centrifugation (500 g for 5 min at 4 °C), and the supernatant was removed. Cells were then fixed and permeabilized in 70 % ethanol at −20 °C. Fixed cells were washed with PBS and incubated in the dark for 30 min with a propidium iodide (PI, BD Pharmingen, CA, USA) staining solution containing 50 mg/ml PI and 100 mg/ml RNaseA in PBS. Flow cytometry analysis was performed using a FACS can flow cytometer (Becton–Dickinson, CA, USA), and data were analyzed using Becton–Dickinson Cell Quest software.

Quantitative RT-PCR

Total RNA was isolated using Trizol reagent (Invitrogen, Carlsbad, CA) according to the manufacturer's instructions. Quantitative RT-PCR was carried out using a Chromo4 instrument (Bio Rad) and a SYBR® Premix Ex Taq™ kit (Takara Bio, Otsu, Japan) to detect mRNA. The specific PCR

primer sequences of these genes, designed using Primer Premier 5.0 software, were as follows: MGMT forward: 5′-CA CTTCACCATCCCGTTTTCC-3′; reverse: 5′-TG CTGGT AAGAAATCACTTCTCC-3′; ABCB1 forward: 5′-GAGGA AGACATGAC CAGGTA-3′; reverse: 5′-CTGTCGCATTA TAGCATGAA-3′; ABCG2 forward: 5′-ACCTGAAGGCA TTTACTGAA-3′; reverse: 5′-TCTTTCCTTGCAGCTAA GA C-3′; CD133 forward: 5′-GCACTCTATACCAAAGCG TCA-3′; reverse: 5′-CCAT ACTTCTTAGTTTCCTCA-3′; Nestin forward: 5′-GAGCAGCACTCTTAACTTA CGA-3′; reverse: 5′-TTCCTACAGCCTCCATTCTTG-3′; GFAP forward: 5′-CGCTGTTTCCCTATCTTC-3′; reverse: 5′-AAT GGGTCGCTGTAATGT-3′; ALDH1 forward: 5′-CCCGT TGGTTATGCTCATTT-3′; reverse: 5′-TGCTCTGC TGGT TTGACAAC-3′; GAPDH forward: 5′-GACCCCTTCATT GACCTCAAC-3′; reverse: 5′-CTTCTCCATGGTGGTGA AGA-3′. Independent experiments were conducted in triplicate. The cycle threshold (Ct), representing a positive PCR result, is defined as the cycle number at which a sample's fluorescence intensity crossed the threshold automatically determined by the Chromo4 system. The relative changes in gene expression were calculated with the $2^{-\Delta\Delta Ct}$ method, where $\Delta\Delta Ct = (Ct_{target\ gene} - Ct_{GAPDH})_{sample} - (Ct_{target\ gene} - Ct_{GAPDH})_{calibrator}$.

Western blotting

For western blot analysis [16], the following antibodies were used: anti-GAPDH, anti-MGMT, anti-α-tubulin, anti-ALDH1, anti-ABCG2, anti-Bcl-2, anti-Bax, anti-c-PARP, anti-Akt, and anti-p-Akt (Cell Signaling Technology, Beverly, MA, USA) at 1:1000; anti-CD133 (BioWorld, USA) at 1:500; anti-P-gp (Santa Cruz Biotechnology, California, USA) at 1:400; and HRP-conjugated secondary antibody (1:5000 dilution; Cell Signaling Technology, Beverly, MA).

Transwell migration assay

For the transwell migration assays, 5×10^3 cells/ml of U87 GSLCs were plated in the top transwell chamber (6.5-mm diameter, 8.0-μm pore size polycarbonate filters; Corning, NY, USA) and allowed to migrate toward serum-containing medium in the lower transwell chamber. After 24 h, the cells were fixed with methanol and stained with 0.1 % crystal violet (2 mg/ml). The number of cells invading through the membrane was counted under a light microscope.

Immunofluorescent staining

Cells were plated on poly-L-lysine-coated coverslips (Sigma) and incubated overnight at 37 °C. Cells were rinsed with PBS and fixed in 3.7 % paraformaldehyde for 10 min. Cells were then washed in PBS three times for 5 min, blocked in 5 % bovine serum albumin for 60 min, then incubated with anti-P-gp antibody (1:200), anti-mouse-FITC secondary antibody (1:1000, Cell Signaling Technology, Beverly, MA), TUNEL reaction mixture containing a nucleotide mixture and terminal deoxynucleotidyl transferase (TdT) (In Situ Cell Death Detection Kit, Roche Diagnostics GmbH, Germany) and 4′,6-diamidino-2-phenylindole (DAPI, Cell Signaling Technology, Beverly, MA). Finally, the slides were mounted and examined by laser scanning confocal microscopy (LSM).

Statistical analysis

All experiments were conducted at least three times. Data from quantitative RT-PCR, IC_{50} values, and the quantification of western blotting results are expressed as the mean $\pm$ standard deviation (SD). Statistical analysis of the EGCG combined with TMZ data was performed using the Kruskal–Wallis test, and analysis of all other data was conducted using a one-way analysis of variance (ANOVA) in the statistical package SPSS 13.0 (SPSS Inc., USA). $P < 0.05$ was considered to be statistically significant.

Results

Generation of GSLCs from U87 sphere culture

Neurosphere culture is a common and convenient method to enrich for GSLCs. Glioma cell line U87 is able to continually divide and form multipotent clonal spheres, so-called neurospheres, after 7 days in selective serum-free media. In suspension, glioma cells accumulate to form globular structures. Neurospheres have a diameter of 150–200 μm. When serum-free medium was replaced with serum-supplemented medium, neurospheres attached to the plate and began proliferating after 3 days (Fig. 1a). Other glioma cell lines (U251MG, C6, SHG-44) also formed neurospheres in selective serum-free media (Fig. 1a). However, only U87 GSLCs could be dissociated with Accutase into a single-cell suspension and subsequently passaged. These results suggest that GSLCs have the capacity for self-renewal and differentiation.

U87 GSLCs exhibit neural stem cell properties

As shown in Fig. 1b, c, the cancer stem cell markers CD133 and ALDH1 were significantly increased in U87 GSLCs compared with U87, whereas the expression of the astrocyte differentiation marker (i.e., GFAP) decreased. However, Nestin expression did not change. Similar results
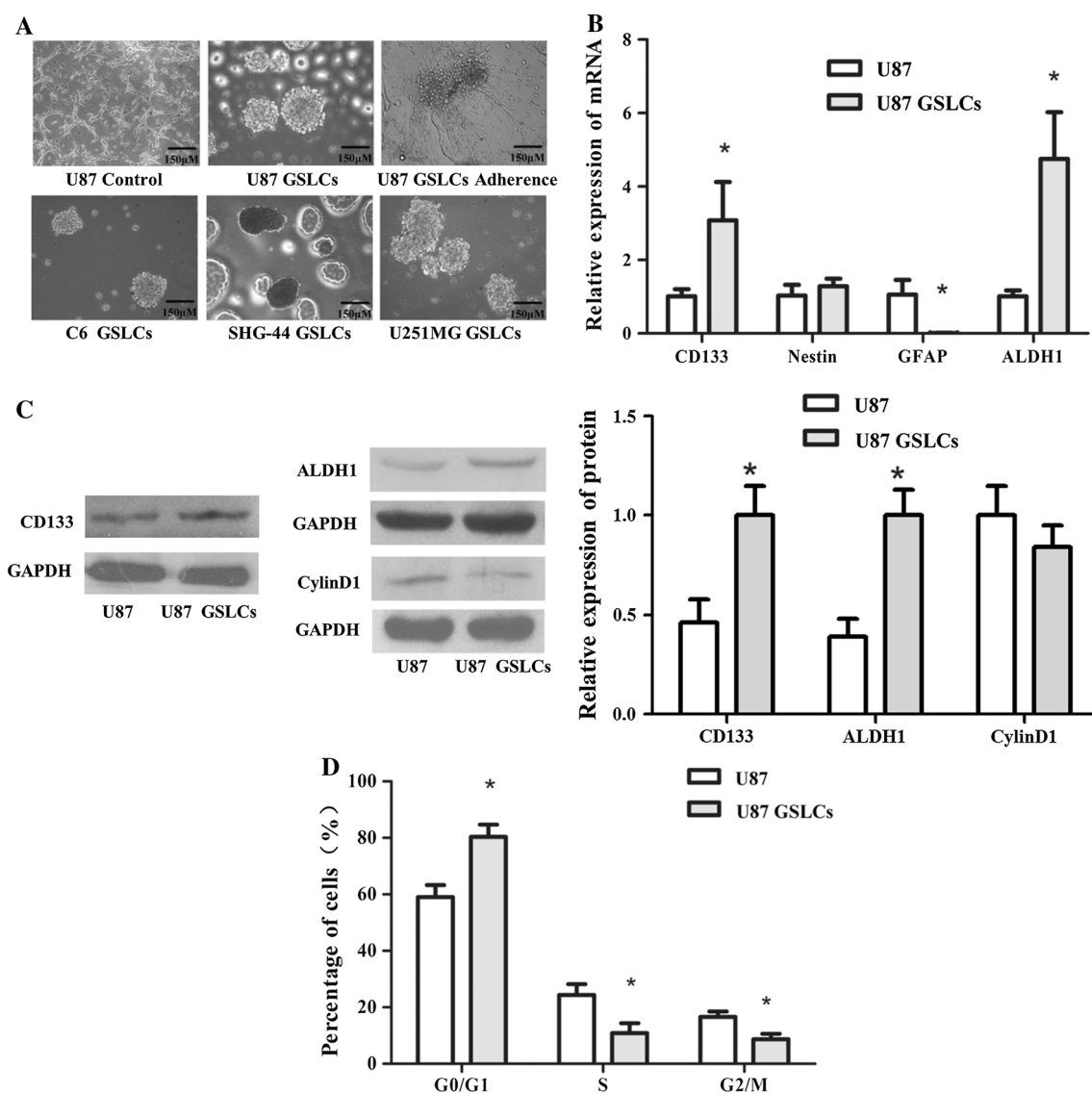
Fig. 1 U87 GSLCs have the properties of neural stem cells when enriched in neurosphere culture. **a** The glioma cell line U87 can form neurospheres. Neurospheres were developed from a monolayer of U87 cells after 7 days in serum-free DMEM/F12 with B-27, EGF, and bFGF supplementation (*middle*). U87 GSLCs attached to the plate and proliferated after 3 days in DMEM/F12 supplemented with 10 % fetal bovine serum (*right*). Normal U87 cells were used as a control (*left*). *Scale bars* 150 μm. The glioma cell lines C6, SHG-44, and U251MG can also form neurospheres in selective serum-free media. **b** mRNA expression levels of ALDH1, Nestin, CD133, and GFAP were detected by RT-PCR and normalized against GAPDH in U87 and U87 GSLCs. **c** CD133, ALDH1 and CylinD1 protein expression was detected using western blotting and normalized against GAPDH in U87 and U87 GSLCs (*left*). The relative fold changes were then calculated (*right*). D The cell cycle was detected using a FACScan flow cytometer in U87 and U87 GSLCs. n = 3. The data represent the mean ± SD. * Significantly different from the respective controls, $P < 0.05$

were observed in C6 GSLCs (Supplementary Fig. 1). Moreover, a higher percentage U87 GSLCs remained in the G0/G1 phase, showing the downregulation of cell cycle protein CylinD1 relative to U87 cells (Fig. 1c, d). These data indicate that U87 GSLCs have characteristics of neural stem cells in terms of their cell cycle and elevated expression of CD133 and ALDH1. Thus, we used this model to further study the effects of EGCG on GSLCs.

U87 GSLCs express higher levels of P-gp and are resistant to BCNU and TMZ

The effect of conventional chemotherapy drugs (BCNU and TMZ) on cell viability in U87 and U87 GSLCs was examined using a CCK-8 assay (Fig. 2a, b). BCNU IC_{50} values in U87 and U87 GSLCs were 1.27 and 21.33 μM, respectively; TMZ values were 260.34 and 766.11 μM,
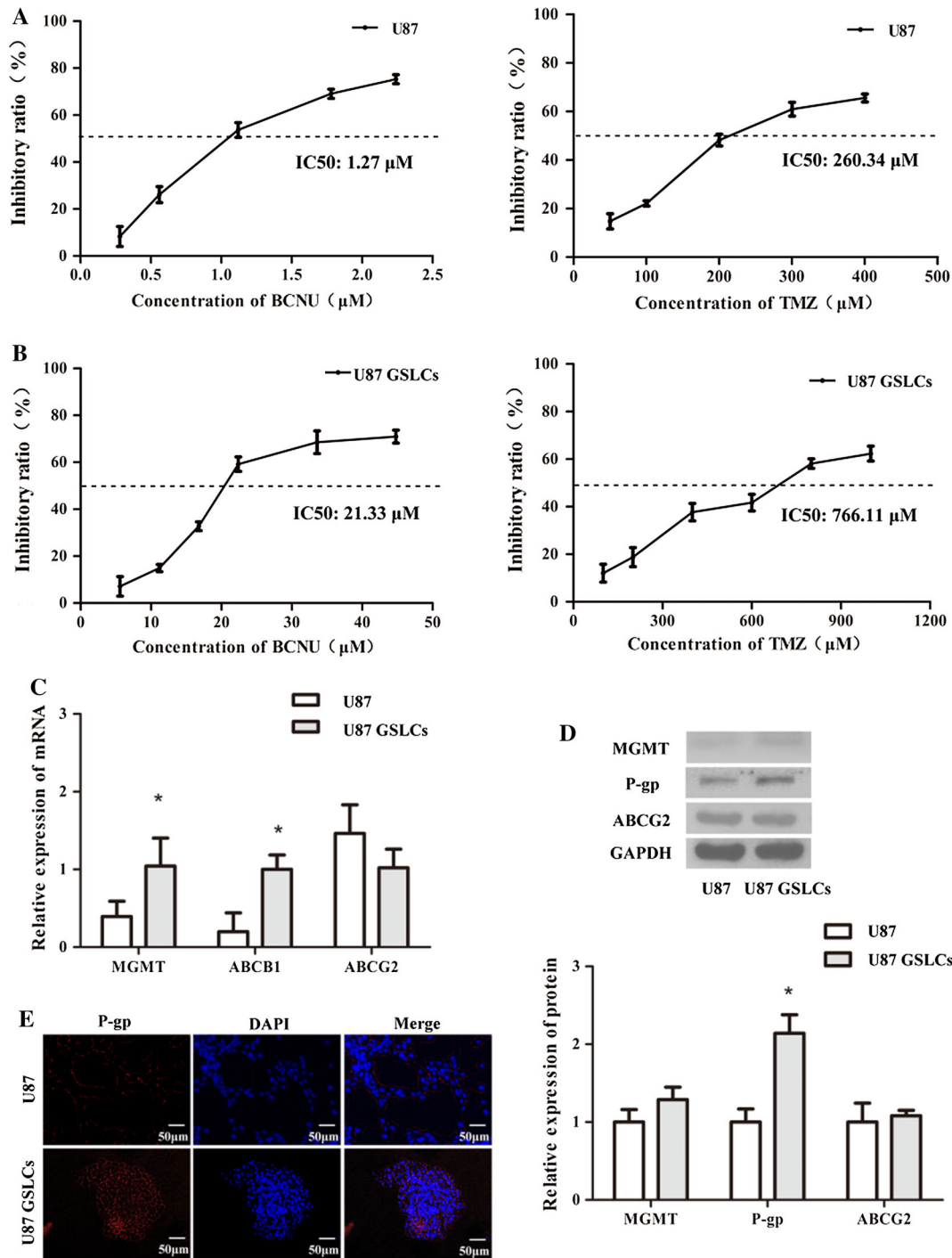
Fig. 2 U87 GSLCs were drug-resistant cells relative to U87. **a, b** Cell viability was assessed using a CCK-8 assay in U87 and U87 GSLCs treated for 24 h with various doses of BCNU and TMZ. **c** mRNA expression levels of MGMT, ABCB1, and ABCG2 were measured by RT-PCR in U87 and U87 GSLCs. **d** MGMT, ABCB1 (P-gp), and ABCG2 protein expression was measured using western blotting (*upper*) and normalized against GAPDH in U87 and U87 GSLCs. Relative fold changes were then calculated (*bottom*). n = 3. Data represent the mean ± SD. * Significantly different from the respective controls, $P < 0.05$. **e** The expression of P-gp in U87 and U87 GSLCs was observed by cell immunofluorescent staining. Blue fluorescence represents DAPI, and red fluorescence represents P-gp. *Scale bars* 50 μm

respectively. The resistance index (RI) of U87 GSLCs for TMZ and BCNU was 3.0 and 16.8, respectively, suggesting that U87 GSLCs may have characteristics of multi-drug resistance. Furthermore, we confirmed that the mRNA and protein expression of the ABCB1 gene was elevated in U87 GSLCs (Fig. 2c, d). A similar result was observed by
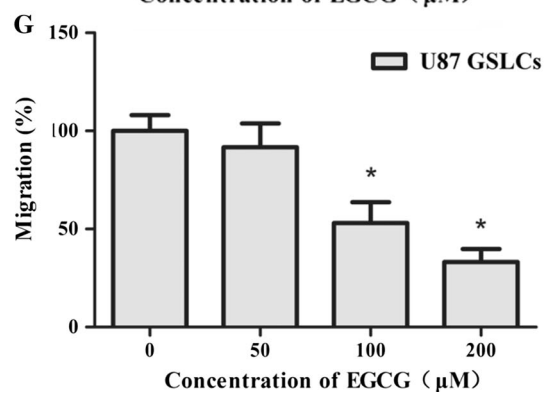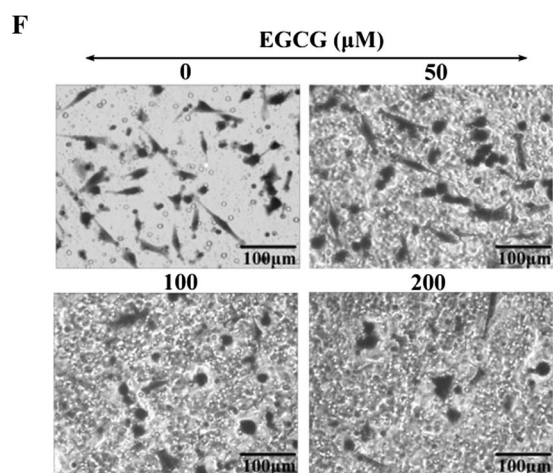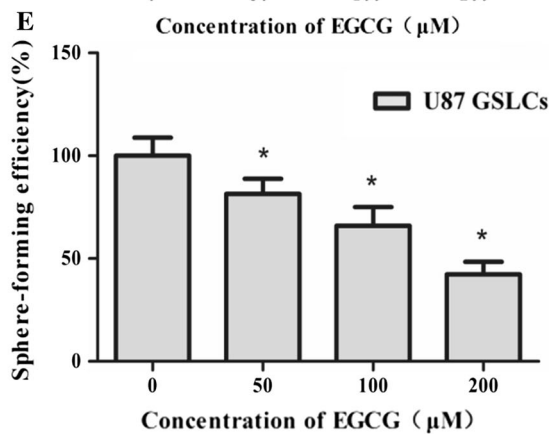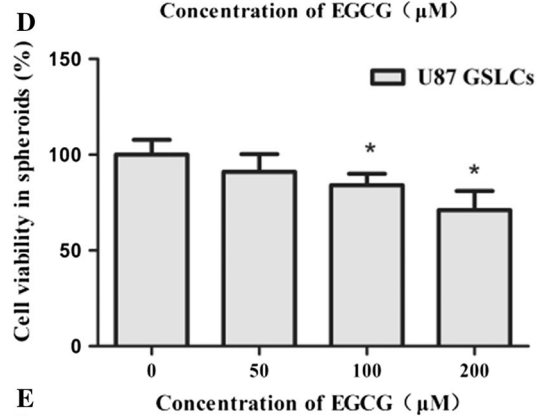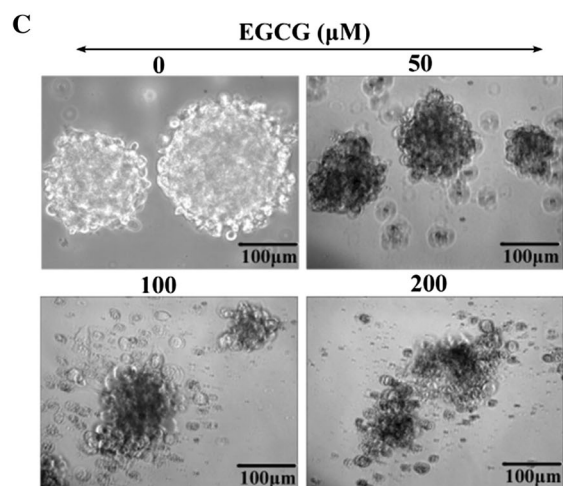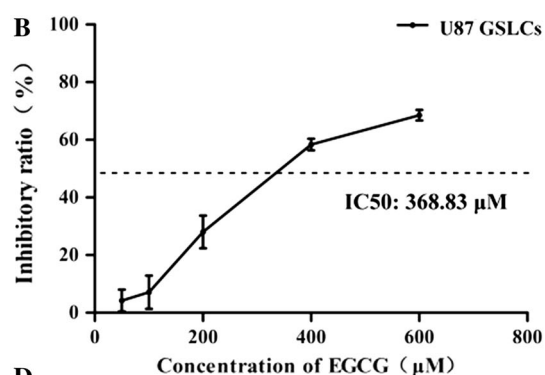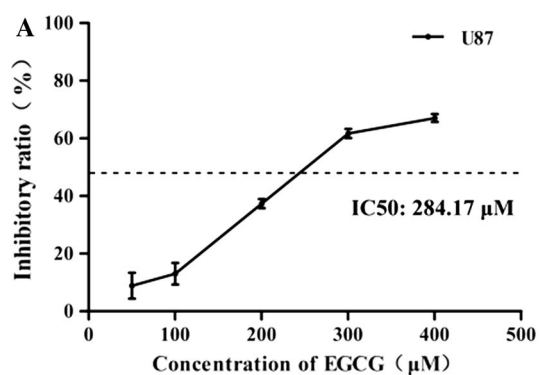
◄**Fig. 3** The inhibitory effects of EGCG on U87 GSLCs include reduced viability, migration, and neurosphere formation. **a**, **b** Cell viability was tested using a CCK-8 assay after treating U87 and U87 GSLCs with various doses of EGCG for 24 h. **c** U87 GSLCs were dissociated with Accutase and filtered through a 40-μm cell strainer. Cells were then seeded in suspension culture and treated with EGCG (0-200 μM) for 7 days in 96-well plates. Pictures of neurospheres in suspension were taken under a microscope. **d** Cell viability was measured using a trypan blue assay; the numbers of live cells were counted under a microscope in five random fields per well. **e** After dissociation, U87 GSLCs were seeded in suspension and treated with EGCG (0–200 μM) for 48 h. Cells were then cultured in serum-free DMEM/F12 supplemented with B-27, EGF, and bFGF for 7 days to check sphere-forming efficiency. The number of U87 GSLCs was counted under a microscope in five random fields per well. Data represent the mean ± SD. * Different from the respective controls, $P < 0.05$. **f** Transwell migration assay. U87 GSLCs at a density of 5,000 cells/ml were plated in the top chamber of the transwell and treated with EGCG (0–200 μM) for 24 h. Cells that migrated to the lower chambers were fixed with methanol and stained with crystal violet. **g** Cells were counted under a microscope in five random fields per well. Data represent the mean ± SD. * Different from the respective controls, $P < 0.05$. *Scale bars* 100 μm

immunofluorescent staining (Fig. 2e). However, MGMT was only upregulated on the mRNA level; based on western blot analysis, MGMT protein was not detected in U87 or U87 GSLCs. Additionally, mRNA and protein expression of ABCG2 did not significantly change in GSLCs (Fig. 2c, d). These data indicate that U87 GSLCs may be BCNU and TMZ-resistant, with elevated expression of P-gp.

## EGCG inhibits cell viability, neurosphere formation, and migration of U87 GSLCs

To investigate whether EGCG could inhibit cell growth in U87 GSLCs, we examined cell viability following EGCG treatment using a CCK-8 assay. EGCG IC_{50} values in U87 and U87 GSLCs were 284.17 μM and 368.83 μM, respectively; there was no significant difference between the values (Fig. 3a, b). The RI of U87 GSLCs with EGCG treatment was 1.3. These data indicate that EGCG may be a useful agent to target drug resistant U87 GSLCs. When U87 GSLCs were dissociated in suspension and treated with EGCG (0–200 μM) for 7 days, we observed a change in cell morphology. EGCG decreased the viability of U87 GSLCs in a dose-dependent manner (Fig. 3c). These data indicate that EGCG may be an effective inhibitor of self-renewal in U87 GSLCs. Additionally, EGCG reduced the efficiency of sphere formation and migration in U87 GSLCs in a dose-dependent manner (Fig. 3e–g). These findings were validated in C6 GSLCs (Supplementary Figs. 2, 3). Our results suggest that the stem-like characteristics of U87 GSLCs can be effectively inhibited by EGCG.

EGCG induces U87 GSLC apoptosis, with downregulation of p-Akt, Bcl-2, and PARP cleavage

To understand the mechanisms underlying the effects of EGCG on U87 GSLCs, we initially assessed the phosphorylation status of Akt. As shown in Fig. 4a, Akt phosphorylation was reduced in response to EGCG in a concentration-dependent manner, but total Akt showed almost no alteration. Moreover, the glioma stem cell (GSC) markers CD133 and ALDH1 were downregulated after EGCG treatment. EGCG was found to upregulate the expression of the apoptosis-promoting protein Bax, downregulate the expression of Bcl-2, and increase the downstream cleavage of PARP in U87 GSLCs (Fig. 4b). The data indicate that EGCG has inhibitory effects on U87 GSLCs, partly through the induction of apoptosis.

EGCG enhances the sensitivity of U87 GSLCs to TMZ and downregulates P-gp

To determine whether the inhibitory effects of EGCG were related to the downregulation of drug-resistance protein, we measured changes in MGMT, ABCB1, and ABCG2 expression in U87 GSLCs. Our data showed that mRNA and protein levels of P-gp were reduced in a dose-dependent manner with EGCG treatment (Fig. 4c, d). However, although MGMT and ABCG2 mRNA expression was reduced with EGCG treatment (Fig. 4c), protein levels did not change. We then evaluated if EGCG in combination with TMZ contributed to the downregulation of P-gp in U87 GSLCs. As shown in Fig. 5a, U87 GSLCs treated with EGCG in combination with TMZ had significantly reduced viability relative to cells treated with EGCG or TMZ alone. Furthermore, although the protein expression of ABCG2 and MGMT did not change significantly after treatment with EGCG and TMZ, P-gp expression in U87 GSLCs was dramatically downregulated (Fig. 5b). A similar result was observed by confocal immunofluorescence staining (Fig. 5c). P-gp expression was decreased in the EGCG and Verapamil (VER) treatment groups relative to the control group, and more apoptotic cells were detected by TUNEL assay. There were no differences in P-gp expression or in the number of apoptotic cells with TMZ treatment. It obviously reduced the expression of P-gp. Apoptotic cells were detected in the TMZ + EGCG treatment group and the VER + EGCG treatment group. Apoptotic cells are indicated by white arrows. Moreover, expression of P-gp in U87 GSLCs and C6 GSLCs was dramatically reduced (Supplementary Figs. 4, 5). These results indicate that EGCG may synergize with TMZ to inhibit P-gp in GSLCs.
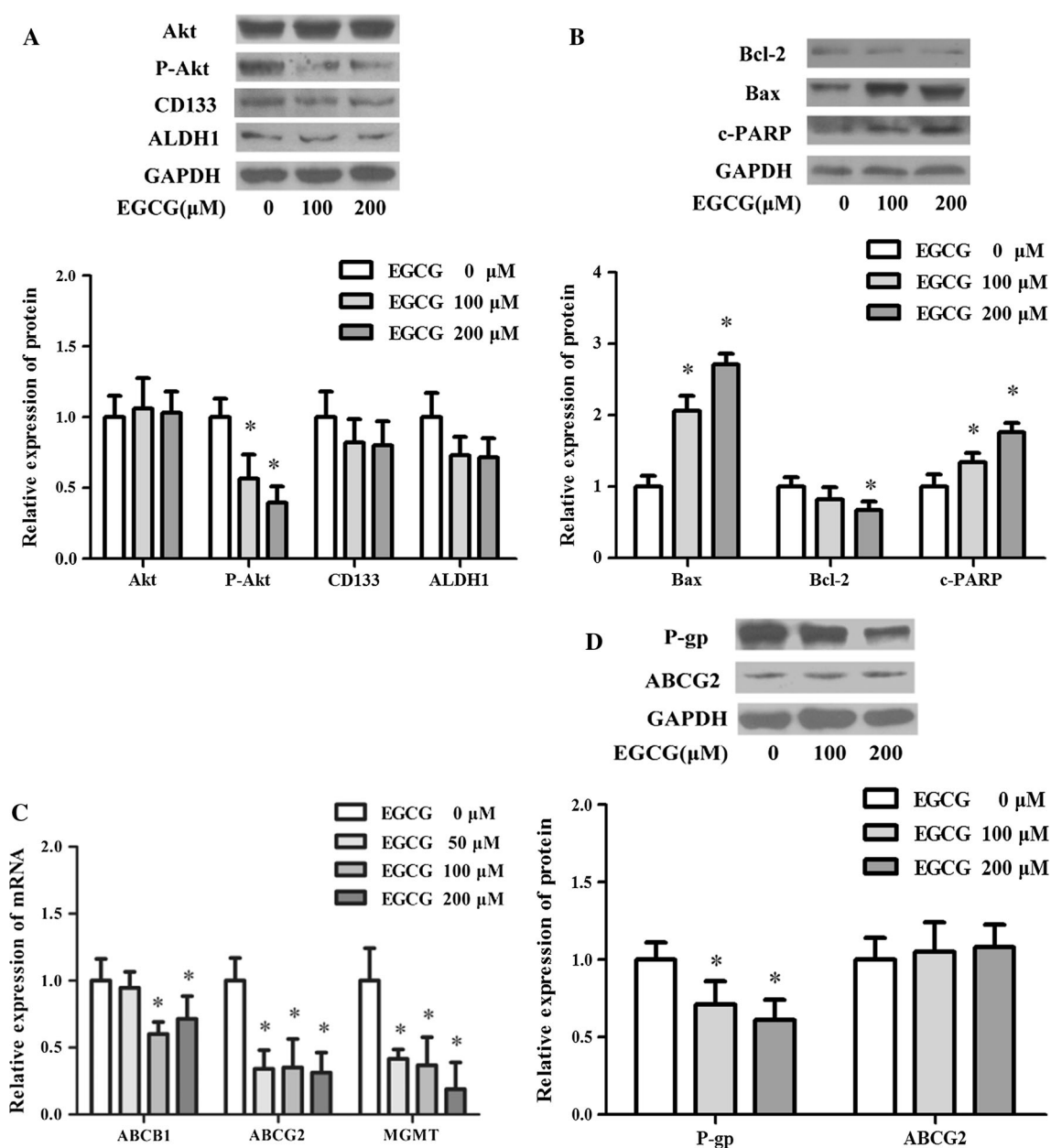
Fig. 4 EGCG downregulates Akt phosphorylation to modulate the Akt signaling pathway, stimulates apoptosis in U87 GSLCs, and downregulates P-gp at the mRNA and protein level. **a** U87 GSLCs were dissociated with Accutase and filtered through a 40-μm cell strainer. The cells were then seeded in suspension and treated with EGCG (0–200 μM) for 24 h. The expression of Akt, P-Akt, CD133 and ALDH1 was measured using western blotting and normalized against GAPDH (upper). Fold changes were calculated (bottom). **b** U87 GSLCs were treated with EGCG (0-200 μM) for 48 h. The expression of Bcl-2, Bax, c-PARP, and GAPDH was measured using western blot analysis (upper). Fold changes were calculated (bottom). **c** U87 GSLCs were seeded in suspension and treated with EGCG (0–200 μM) for 24 h. The mRNA expression levels of MGMT, ABCB1, and ABCG2 were measured by RT-PCR and normalized against GAPDH. **d** The expression of MGMT, ABCB1 (P-gp), and ABCG2 was measured using western blotting and normalized against GAPDH (upper). Fold changes were calculated (bottom). Data represent the mean ± SD. * Different from the respective controls, $P < 0.05$

Discussion

Clinical resistance to chemotherapeutic drugs is a serious problem in glioma treatment. GSCs are potentially important because they are likely to express high levels of drug-resistance proteins and are often responsible for recurrences after glioma treatment. In this study, we enriched for cells with stem-like characteristics and identified U87 GSLCs as high expressors of CD133, ALDH1 and P-gp. Importantly, we show for the first time that EGCG
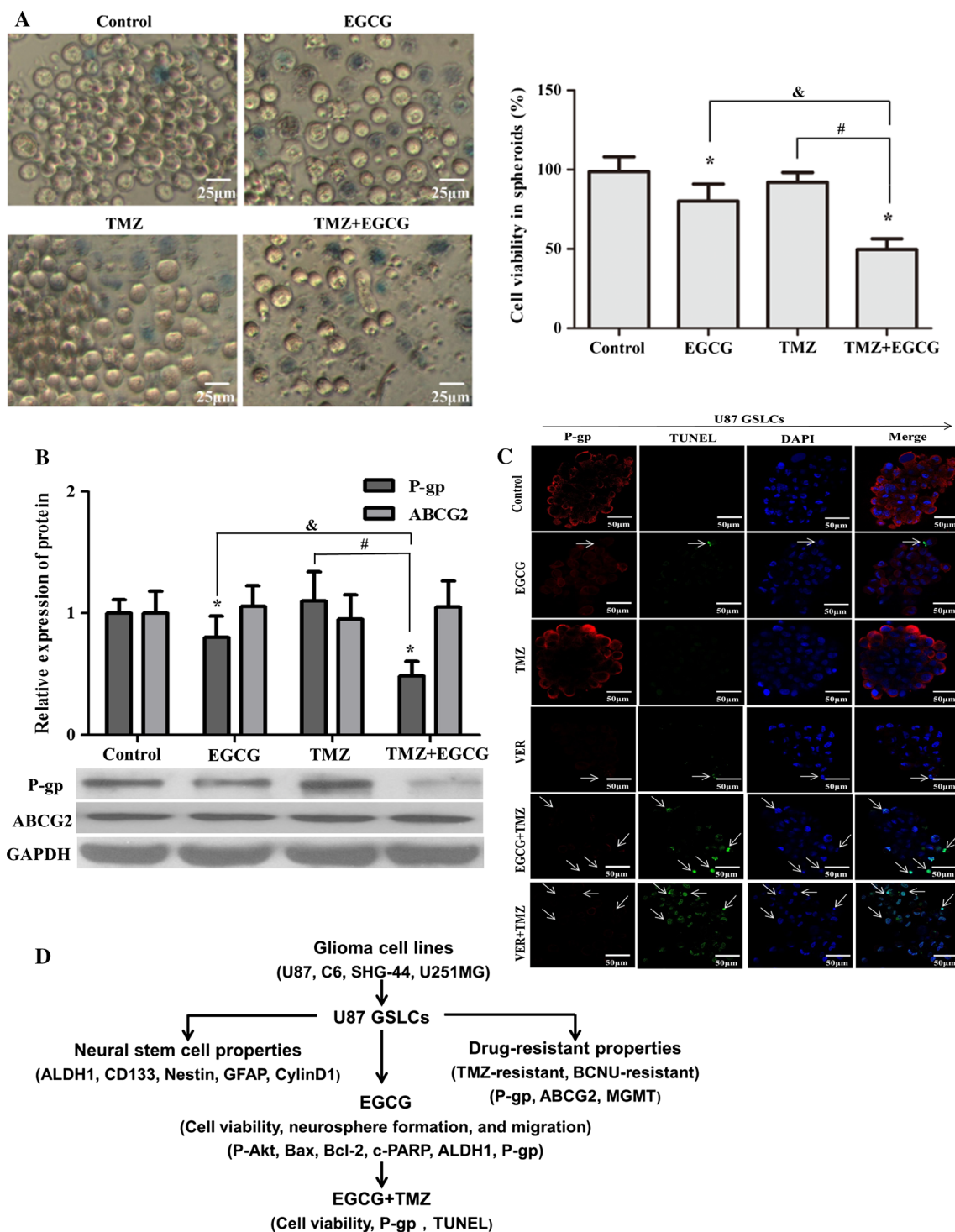
Fig. 5 EGCG enhances sensitivity to P-glycoprotein-mediated multidrug resistance when combined with TMZ in U87 GSLCs. **a** U87 GSLCs were seeded in suspension and treated with the control, 100 μM EGCG, 100 μM TMZ, or TMZ combined with EGCG for 48 h. Cells were then dissociated with Accutase and treated with trypan blue dye (*left*). Cell viability was calculated by counting live cells under a microscope in five random fields per well (*right*). Data represent the mean ± SD. * Different from the respective controls, #,& Significant difference between the two connected objects, Kruskal–Wallis test, $P < 0.05$. *Scale bars* 25 μm. **b** In the same treatment conditions, MGMT, ABCB1 (P-gp), and ABCG2 expression levels were measured using western blotting (*bottom*). Fold changes were calculated (*upper*). Data represent the mean ± SD. * Different from the respective controls, #,& Significant difference between the two connected objects, Kruskal–Wallis test, $P < 0.05$. **c** Confocal immunofluorescence staining. U87 GSLCs were seeded in suspension and treated with control, 100 μM EGCG, 100 μM TMZ, 50 μM VER, EGCG + TMZ, or VER + TMZ for 48 h. Blue fluorescence represents DAPI, red fluorescence represents P-gp, and green fluorescence represents TUNEL. Apoptotic cells are indicated by *white arrows*. *Scale bars* 50 μm. **d** Schematic overview of the anti-cancer action of EGCG alone or in combination with TMZ in U87 GSLCs

can inhibit GSLC viability, neurosphere formation, migration and inducing apoptosis. We also demonstrated that EGCG sensitized GSLCs to temozolomide; this phenomenon was associated with downregulation of P-gp in vitro (Fig. 5d). These results demonstrate that EGCG can be used for the management of GSCs.

Several methods are currently in use to establish GSC models, including neurosphere culture, flow cytometer sorting based on surface markers, and side population (SP) assays [17–19]. Normally, these GSCs exhibit characteristics similar to normal stem cells; this includes remaining quiescent during the cell cycle as a result of their capacity for perpetual self-renewal and a wide differentiation potential [20]. Microenvironmental factors and the activation of specific signaling pathways are able to sustain the small population of remaining GSCs [21]. Neurosphere culture is the most convenient method for enriching GSCs because it provides a microenvironment that promotes the proliferation of stem-like cells [22]. Using neurosphere culture, we enriched for GSLCs from four glioma cell lines (U87, C6, SHG-44, and U251MG) and found that U87 GSLCs were easier to resuspend with Accutase and more convenient to subculture (Fig. 1a). In addition, our supplemental results demonstrate that C6 GSLCs were easier to resuspend with TrypLE Express reagent (another stem cell digestive enzyme) for subculturing.

Several cancer stem cell markers have been used to identify GSCs. Recently, a CD133(+) or ALDH1(+) subpopulation isolated from human brain tumors was shown to exhibit stem cell properties and thought to play a pivotal role in brain tumor initiation, growth, and recurrence [23, 24]. Likewise, ALDH1 is a common stem cell marker in many other cancer cells, including malignant human epithelium, prostate, and colon [25–28]. Additionally, neural stem cells usually remain quiescent by downregulating CylinD1 [29]. Consistent with other studies [30], our results show that U87 GSLCs express CD133 and ALDH1 at high levels, and remained at the G0/G1 phase with downregulation of CylinD1; this suggests that we succeeded in enriching and identifying U87 GSLCs with the properties of cancer stem cells.

Recent studies have reported that EGCG inhibits several stem-like cells, including nasopharyngeal, breast, prostate, and pancreatic cancer stem cells [31–35]. Here, we found that EGCG reduced both U87 and C6 GSLC viability, neurosphere formation, and migration (Fig. 3c–g; Supplementary Fig. 3). We also found that EGCG induced apoptosis in U87 GSLCs by the reducing Akt phosphorylation, inactivating anti-apoptotic protein Bcl-2, upregulating the apoptosis-promoting protein Bax, and cleaving PARP. This result is in agreement with the finding that EGCG can inhibit PI3K and/or mTOR kinases to target the PI3K/Akt/mTOR pathway in several cancer cells [36]. The

PI3K/Akt/Bcl-2 signaling pathway plays a critical role in regulating cellular proliferation and apoptosis [37–39]. Moreover, gliomas are sensitive to apoptosis through the downregulation of anti-apoptotic Bcl-2 family members [40, 41]. These data suggest that EGCG may be an effective agent to target GSLCs associated with inhibition of an Akt-related pathway.

TMZ is a recently launched anti-glioma drug, but high expression of resistance proteins reduces its efficacy [42]. In this study, we found that EGCG enhanced the sensitivity of U87 GSLCs to TMZ and significantly downregulated the expression of P-gp, but not ABCG2 or MGMT (Fig. 4c, d). EGCG treatment significantly downregulated transcript levels of ABCG2 and MGMT, but not protein levels; this is in contrast to ABCB1/P-gp, suggesting that ABCG2 and MGMT may be regulated at not only the transcriptional level but also post-translational and protein stability levels. Previous studies have shown that MGMT is protective against cell death induced by alkylating agents, such as BCNU and TMZ [43]. Our data show that MGMT protein expression was marginal in U87 and U87 GSLCs, consistent with previous studies [44, 45]. Chen et al. reported that EGCG enhanced the therapeutic efficacy of TMZ by inhibiting GRP78 in mouse glioblastoma models [46]. Qian et al. reported that EGCG modulated the function of P-gp and reversed multidrug resistance in cancer cells [47]. As reported, VER and talinolol are substrates of P-gp and mitoxantrone and topotecan are substrates of ABCG2. Rhodamine 123 and [³H] daunorubicin are shared substrates of P-gp and ABCG2 [48]. Jodoin et al. suggested that EGCG was a competitive inhibitor of P-gp [49]. This P-gp inhibition may be associated with tight binding of EGCG to the ATP-binding site, resulting in an enhancement of the effects of the substrate of P-gp. Therefore, EGCG may enhance sensitivity to TMZ by modulating P-gp and other resistance-associated proteins. We did not observe downregulation of P-gp with TMZ treatment, which is inconsistent with the findings of Riganti et al. [50]. This is possibly because we used TMZ under more moderate experimental conditions, including lower concentrations and shorter treatment times. We found that the decrease in P-gp expression and increase in apoptosis in the TMZ + EGCG group was similar observations our in the VER + EGCG group. This suggests that EGCG synergized with TMZ and may be associated with P-gp inhibition (Fig. 5c; Supplementary Fig. 5). Additional studies in other GSC cell lines or patients will be necessary to further explore the synergistic effects of EGCG and TMZ in vitro and in vivo.

In conclusion, we observed for the first time that EGCG reduces cell viability and migration in U87 GSLCs. It also stimulated apoptosis, downregulating Bcl-2, Akt phosphorylation, and cleaving PARP in a dose-dependent

manner. More importantly, EGCG enhanced sensitivity to TMZ, associated with inhibition of P-gp. This study provides new insights into GSC-based anti-glioma treatments and EGCG development.

References

1. Sarkaria JN, Kitange GJ, James CD, Plummer R, Calvert H, Weller M, Wick W (2008) Mechanisms of chemoresistance to alkylating agents in malignant glioma. Clin Cancer Res 14:2900–2908. doi:10.1158/1078-0432.CCR-07-1719
2. Sai K, Yang QY, Shen D, Chen ZP (2013) Chemotherapy for gliomas in mainland China: an overview. Oncol Lett 5:1448–1452. doi:10.3892/ol.2013.1264
3. Galli R, Binda E, Orfanelli U, Cipelletti B, Gritti A, De Vitis S, Fiocco R, Foroni C, Dimeco F, Vescovi A (2004) Isolation and characterization of tumorigenic, stem-like neural precursors from human glioblastoma. Cancer Res 64:7011–7021. doi:10.1158/0008-5472.CAN-04-1364
4. Christmann M, Verbeek B, Roos WP, Kaina B (2011) O(6)-Methylguanine-DNA methyltransferase (MGMT) in normal tissues and tumors: enzyme activity, promoter methylation and immunohistochemistry. Biochim Biophys Acta 1816:179–190. doi:10.1016/j.bbcan.2011.06.002
5. Nakai E, Park K, Yawata T, Chihara T, Kumazawa A, Nakabayashi H, Shimizu K (2009) Enhanced MDR1 expression and chemoresistance of cancer stem cells derived from glioblastoma. Cancer Invest 27:901–908. doi:10.3109/07357900801946679
6. Yin BB, Wu SJ, Zong HJ, Ma BJ, Cai D (2011) Preliminary screening and identification of stem cell-like sphere clones in a gallbladder cancer cell line GBC-SD. J Zhejiang Univ Sci B 12:256–263. doi:10.1631/jzus.B1000303
7. Imai Y, Tsukahara S, Asada S, Sugimoto Y (2004) Phytoestrogens/flavonoids reverse breast cancer resistance protein/ABCG2-mediated multidrug resistance. Cancer Res 64:4346–4352. doi:10.1158/0008-5472.CAN-04-0078
8. Shi Z, Liang YJ, Chen ZS, Wang XW, Wang XH, Ding Y, Chen LM, Yang XP, Fu LW (2006) Reversal of MDR1/P-glycoprotein-mediated multidrug resistance by vector-based RNA interference in vitro and in vivo. Cancer Biol Ther 5:39–47
9. Vlachostergios PJ, Hatzidaki E, Befani CD, Liakos P, Papandreou CN (2013) Bortezomib overcomes MGMT-related resistance of glioblastoma cell lines to temozolomide in a schedule-dependent manner. Invest New Drugs. doi:10.1007/s10637-013-9968-1
10. Singh BN, Shankar S, Srivastava RK (2011) Green tea catechin, epigallocatechin-3-gallate (EGCG): mechanisms, perspectives and clinical applications. Biochem Pharmacol 82:1807–1821. doi:10.1016/j.bcp.2011.07.093
11. Shankar S, Ganapathy S, Srivastava RK (2007) Green tea polyphenols: biology and therapeutic implications in cancer. Front Biosci 12:4881–4899
12. Chen H, Landen CN, Li Y, Alvarez RD, Tollefsbol TO (2013) Epigallocatechin gallate and sulforaphane combination treatment induce apoptosis in paclitaxel-resistant ovarian cancer cells through hTERT and Bcl-2 down-regulation. Exp Cell Res 319:697–706. doi:10.1016/j.yexcr.2012.12.026
13. Sadava D, Whitlock E, Kane SE (2007) The green tea polyphenol, epigallocatechin-3-gallate inhibits telomerase and induces apoptosis in drug-resistant lung cancer cells. Biochem Biophys Res Commun 360:233–237. doi:10.1016/j.bbrc.2007.06.030
14. Farabegoli F, Papi A, Bartolini G, Ostan R, Orlandi M (2010) (-)-Epigallocatechin-3-gallate downregulates Pg-P and BCRP in a tamoxifen resistant MCF-7 cell line. Phytomedicine 17:356–362. doi:10.1016/j.phymed.2010.01.001
15. Huang HY, Niu JL, Zhao LM, Lu YH (2011) Reversal effect of 2′,4′-dihydroxy-6′-methoxy-3′,5′-dimethylchalcone on multidrug resistance in resistant human hepatocellular carcinoma cell line BEL-7402/5-FU. Phytomedicine 18:1086–1092. doi:10.1016/j.phymed.2011.04.001
16. Burnette WN (1981) "Western blotting": electrophoretic transfer of proteins from sodium dodecyl sulfate–polyacrylamide gels to unmodified nitrocellulose and radiographic detection with antibody and radioiodinated protein A. Anal Biochem 112:195–203
17. Wan F, Zhang S, Xie R, Gao B, Campos B, Herold-Mende C, Lei T (2010) The utility and limitations of neurosphere assay, CD133 immunophenotyping and side population assay in glioma stem cell research. Brain Pathol 20:877–889. doi:10.1111/j.1750-3639.2010.00379.x
18. Chaichana K, Zamora-Berridi G, Camara-Quintana J, Quinones-Hinojosa A (2006) Neurosphere assays: growth factors and hormone differences in tumor and nontumor studies. Stem Cells 24:2851–2857. doi:10.1634/stemcells.2006-0399
19. Patrawala L, Calhoun T, Schneider-Broussard R, Zhou J, Claypool K, Tang DG (2005) Side population is enriched in tumorigenic, stem-like cancer cells, whereas ABCG2+ and ABCG2− cancer cells are similarly tumorigenic. Cancer Res 65:6207–6219. doi:10.1158/0008-5472.CAN-05-0592
20. Venezia TA, Merchant AA, Ramos CA, Whitehouse NL, Young AS, Shaw CA, Goodell MA (2004) Molecular signatures of proliferation and quiescence in hematopoietic stem cells. PLoS Biol 2:e301. doi:10.1371/journal.pbio.0020301
21. Persano L, Rampazzo E, Basso G, Viola G (2013) Glioblastoma cancer stem cells: role of the microenvironment and therapeutic targeting. Biochem Pharmacol 85:612–622. doi:10.1016/j.bcp.2012.10.001
22. Mori H, Ninomiya K, Kino-oka M, Shofuda T, Islam MO, Yamasaki M, Okano H, Taya M, Kanemura Y (2006) Effect of neurosphere size on the growth rate of human neural stem/progenitor cells. J Neurosci Res 84:1682–1691. doi:10.1002/jnr.21082
23. Tabatabai G, Weller M (2011) Glioblastoma stem cells. Cell Tissue Res 343:459–465. doi:10.1007/s00441-010-1123-0
24. Singh SK, Clarke ID, Terasaki M, Bonn VE, Hawkins C, Squire J, Dirks PB (2003) Identification of a cancer stem cell in human brain tumors. Cancer Res 63:5821–5828
25. Deng S, Yang X, Lassus H, Liang S, Kaur S, Ye Q, Li C, Wang LP, Roby KF, Orsulic S, Connolly DC, Zhang Y, Montone K, Butzow R, Coukos G, Zhang L (2010) Distinct expression levels and patterns of stem cell marker, aldehyde dehydrogenase isoform 1 (ALDH1), in human epithelial cancers. PLoS One 5:e10277. doi:10.1371/journal.pone.0010277
26. Ginestier C, Hur MH, Charafe-Jauffret E, Monville F, Dutcher J, Brown M, Jacquemier J, Viens P, Kleer CG, Liu S, Schott A, Hayes D, Birnbaum D, Wicha MS, Dontu G (2007) ALDH1 is a marker of normal and malignant human mammary stem cells and a predictor of poor clinical outcome. Cell Stem Cell 1:555–567. doi:10.1016/j.stem.2007.08.014
27. Li T, Su Y, Mei Y, Leng Q, Leng B, Liu Z, Stass SA, Jiang F (2010) ALDH1A1 is a marker for malignant prostate stem cells

and predictor of prostate cancer patients' outcome. Lab Invest 90:234–244. doi:10.1038/labinvest.2009.127

28. Huang EH, Hynes MJ, Zhang T, Ginestier C, Dontu G, Appelman H, Fields JZ, Wicha MS, Boman BM (2009) Aldehyde dehydrogenase 1 is a marker for normal and malignant human colonic stem cells (SC) and tracks SC overpopulation during colon tumorigenesis. Cancer Res 69:3382–3389. doi:10.1158/0008-5472.CAN-08-4418

29. Zang Y, Yu LF, Nan FJ, Feng LY, Li J (2009) AMP-activated protein kinase is involved in neural stem cell growth suppression and cell cycle arrest by 5-aminoimidazole-4-carboxamide-1-beta-D-ribofuranoside and glucose deprivation by down-regulating phospho-retinoblastoma protein and cyclin D. J Biol Chem 284:6175–6184. doi:10.1074/jbc.M806887200

30. Zhao S, Liu H, Liu Y, Wu J, Wang C, Hou X, Chen X, Yang G, Zhao L, Che H, Bi Y, Wang H, Peng F, Ai J (2013) miR-143 inhibits glycolysis and depletes stemness of glioblastoma stem-like cells. Cancer Lett 333:253–260. doi:10.1016/j.canlet.2013.01.039

31. Lin CH, Shen YA, Hung PH, Yu YB, Chen YJ (2012) Epigallocathechin gallate, polyphenol present in green tea, inhibits stem-like characteristics and epithelial-mesenchymal transition in nasopharyngeal cancer cell lines. BMC Complement Altern Med 12:201. doi:10.1186/1472-6882-12-201

32. Lee SH, Nam HJ, Kang HJ, Kwon HW, Lim YC (2013) Epigallocatechin-3-gallate attenuates head and neck cancer stem cell traits through suppression of Notch pathway. Eur J Cancer. doi:10.1016/j.ejca.2013.06.025

33. Chen D, Pamu S, Cui Q, Chan TH, Dou QP (2012) Novel epigallocatechin gallate (EGCG) analogs activate AMP-activated protein kinase pathway and target cancer stem cells. Bioorg Med Chem 20:3031–3037. doi:10.1016/j.bmc.2012.03.002

34. Tang SN, Fu J, Nall D, Rodova M, Shankar S, Srivastava RK (2012) Inhibition of sonic hedgehog pathway and pluripotency maintaining factors regulate human pancreatic cancer stem cell characteristics. Int J Cancer 131:30–40. doi:10.1002/ijc.26323

35. Tang SN, Singh C, Nall D, Meeker D, Shankar S, Srivastava RK (2010) The dietary bioflavonoid quercetin synergizes with epigallocathechin gallate (EGCG) to inhibit prostate cancer stem cell characteristics, invasion, migration and epithelial-mesenchymal transition. J Mol Signal 5:14. doi:10.1186/1750-2187-5-14

36. Van Aller GS, Carson JD, Tang W, Peng H, Zhao L, Copeland RA, Tummino PJ, Luo L (2011) Epigallocatechin gallate (EGCG), a major component of green tea, is a dual phosphoinositide-3-kinase/mTOR inhibitor. Biochem Biophys Res Commun 406:194–199. doi:10.1016/j.bbrc.2011.02.010

37. Premkumar DR, Jane EP, DiDomenico JD, Vukmer NA, Agostino NR, Pollack IF (2012) ABT-737 synergizes with bortezomib to induce apoptosis, mediated by Bid cleavage, Bax activation, and mitochondrial dysfunction in an Akt-dependent context in malignant human glioma cell lines. J Pharmacol Exp Ther 341:859–872. doi:10.1124/jpet.112.191536

38. Chen NG, Lu CC, Lin YH, Shen WC, Lai CH, Ho YJ, Chung JG, Lin TH, Lin YC, Yang JS (2011) Proteomic approaches to study epigallocatechin gallate-provoked apoptosis of TSGH-8301 human urinary bladder carcinoma cells: roles of AKT and heat shock protein 27-modulated intrinsic apoptotic pathways. Oncol Rep 26:939–947. doi:10.3892/or.2011.1377

39. Liu D, Li P, Song S, Liu Y, Wang Q, Chang Y, Wu Y, Chen J, Zhao W, Zhang L, Wei W (2012) Pro-apoptotic effect of epi-gallo-catechin-3-gallate on B lymphocytes through regulating BAFF/PI3 K/Akt/mTOR signaling in rats with collagen-induced arthritis. Eur J Pharmacol 690:214–225. doi:10.1016/j.ejphar.2012.06.026

40. Li C, Zhou C, Wang S, Feng Y, Lin W, Lin S, Wang Y, Huang H, Liu P, Mu YG, Shen X (2011) Sensitization of glioma cells to tamoxifen-induced apoptosis by Pl3-kinase inhibitor through the GSK-3beta/beta-catenin signaling pathway. PLoS One 6:e27053. doi:10.1371/journal.pone.0027053

41. Manero F, Gautier F, Gallenne T, Cauquil N, Gree D, Cartron PF, Geneste O, Gree R, Vallette FM, Juin P (2006) The small organic compound HA14-1 prevents Bcl-2 interaction with Bax to sensitize malignant glioma cells to induction of cell death. Cancer Res 66:2757–2764. doi:10.1158/0008-5472.CAN-05-2097

42. Bleau AM, Huse JT, Holland EC (2009) The ABCG2 resistance network of glioblastoma. Cell Cycle 8:2936–2944

43. Liu L, Gerson SL (2006) Targeted modulation of MGMT: clinical implications. Clin Cancer Res 12:328–331. doi:10.1158/1078-0432.CCR-05-2543

44. Chahal M, Xu Y, Lesniak D, Graham K, Famulski K, Christensen JG, Aghi M, Jacques A, Murray D, Sabri S, Abdulkarim B (2010) MGMT modulates glioblastoma angiogenesis and response to the tyrosine kinase inhibitor sunitinib. Neuro Oncol 12:822–833. doi:10.1093/neuonc/noq017

45. Ryu CH, Yoon WS, Park KY, Kim SM, Lim JY, Woo JS, Jeong CH, Hou Y, Jeun SS (2012) Valproic acid downregulates the expression of MGMT and sensitizes temozolomide-resistant glioma cells. J Biomed Biotechnol 2012:987495. doi:10.1155/2012/987495

46. Chen TC, Wang W, Golden EB, Thomas S, Sivakumar W, Hofman FM, Louie SG, Schonthal AH (2011) Green tea epigallocatechin gallate enhances therapeutic efficacy of temozolomide in orthotopic mouse glioblastoma models. Cancer Lett 302:100–108. doi:10.1016/j.canlet.2010.11.008

47. Qian F, Wei D, Zhang Q, Yang S (2005) Modulation of P-glycoprotein function and reversal of multidrug resistance by (−)-epigallocatechin gallate in human cancer cells. Biomed Pharmacother 59:64–69. doi:10.1016/j.biopha.2005.01.002

48. Weksler BB, Subileau EA, Perriere N, Charneau P, Holloway K, Leveque M, Tricoire-Leignel H, Nicotra A, Bourdoulous S, Turowski P, Male DK, Roux F, Greenwood J, Romero IA, Couraud PO (2005) Blood-brain barrier-specific properties of a human adult brain endothelial cell line. FASEB J 19:1872–1874. doi:10.1096/fj.04-3458fje

49. Jodoin J, Demeule M, Beliveau R (2002) Inhibition of the multidrug resistance P-glycoprotein activity by green tea polyphenols. Biochim Biophys Acta 1542:149–159

50. Riganti C, Salaroglio IC, Caldera V, Campia I, Kopecka J, Mellai M, Annovazzi L, Bosia A, Ghigo D, Schiffer D (2013) Temozolomide downregulates P-glycoprotein expression in glioblastoma stem cells by interfering with the Wnt3a/glycogen synthase-3 kinase/beta-catenin pathway. Neuro Oncol. doi:10.1093/neuonc/not104